

Luttinger liquid properties of the steady state after a quantum quench

D.M. Kennes and V. Meden

*Institut für Theorie der Statistischen Physik, RWTH Aachen University and
JARA—Fundamentals of Future Information Technology, 52056 Aachen, Germany*

(Dated: April 23, 2013)

We study the dynamics resulting out of an abrupt change of the two-particle interaction in models of closed one-dimensional Fermi systems: the field theoretical Tomonaga-Luttinger model and a microscopic lattice model. Using a nonperturbative approach which is controlled for small two-particle interactions we are able to reach large times allowing us to access the properties of the steady state of the lattice model. Comparing those to the exact solution of the full dynamics in the Tomonaga-Luttinger model we provide evidence for universal Luttinger liquid behavior. We show that a single impurity leads to open and perfect chain fixed points in the steady state similar to the ones found in equilibrium [Phys. Rev. Lett. **68**, 1220 (1992)].

PACS numbers: 71.10.Pm, 02.30.Ik, 03.75.Ss, 05.70.Ln

With the rapid progress in the preparation and measurement techniques for isolated cold gases [1] investigating the fundamental questions of if and how a closed quantum many-body system prepared in a nonequilibrium initial state approaches a stationary one is within experimental reach. Studying the physics of the steady state itself is of particular interest if it is nonthermal [2], that is expectation values of observables differ from those computed using a canonical statistical operator with the temperature fixed by the excess energy. One-dimensional (1d) interacting Fermi systems are promising candidates for realizing such unusual nonequilibrium states as in many of those the dynamics is restricted not only by energy conservation but by several additional conservation laws [3]. An often studied protocol is an abrupt parameter quench. The system is prepared in the canonical ensemble of an initial Hamiltonian $H(U_i)$. The time evolution is performed with $H(U_f)$, $U_f \neq U_i$. After taking the thermodynamic limit a finite subsystem [4] or local observables [5] might become stationary and describable by a time independent statistical operator. In our case the quenching parameter U is the amplitude of the two-particle interaction.

Interacting 1d quantum systems are exceptional for a different reason as well [6, 7]. The equilibrium low-energy properties of generic models are not described by a Fermi liquid theory. Instead of being fermionic quasi-particles, the gapless elementary excitations are of bosonic nature. Systems of this type fall into the Luttinger liquid (LL) universality class [8]. The observation that the field theoretical Tomonaga-Luttinger (TL) model is the infrared fixed point of a large class of models under a renormalization group (RG) flow lies at the heart of the equilibrium LL concept [9]. For the case of spinless models the fixed point is characterized by the velocity v of the collective excitations and the LL parameter K entering exponents of algebraically decaying correlation functions. Both depend on the parameters of a given model, in particular on U . Alternatively, the two-particle interaction might

open a gap, a situation we do not consider here.

One of the hallmarks of LLs is their sensitivity towards inhomogeneities. For repulsive interactions with $K < 1$ the density response function of a LL diverges as [10] $\chi(q, \omega = 0) \sim |q - 2k_F|^{2K-2}$, with the Fermi momentum k_F . This indicates that even a single weak impurity acts as a strong perturbation. In fact, the homogeneous perfect chain fixed point turned out to be unstable [11–13]. The system flows towards an open chain one with dramatic consequences for the equilibrium low-energy properties; e.g. the linear conductance vanishes as $G \sim T^{2K-1-2}$ for temperature $T \rightarrow 0$.

In this Letter we achieve two distinct goals. (i) We show that the *steady state* of a microscopic 1d lattice model after an interaction quench is characterized by the same power laws as the TL model after a similar quench [14–19] with the K taken for the respective model. As the concept of RG irrelevance cannot directly be transferred to nonequilibrium [16, 19, 20] this is a highly nontrivial result which complements earlier indications of LL universality in the *time evolution towards the steady state* [21]. (ii) We study the physics of a single impurity in the nonequilibrium steady-state LL. For $K < 1$ a stable open and an unstable perfect chain fixed point is found, in analogy to equilibrium [11]. We determine the power-law scaling of the conductance as a function of T . The data for different impurity amplitudes fall on a one-parameter scaling curve indicating the absence of any additional fixed points. The dynamics of the TL model is solved exactly using bosonization [6, 7, 22]. To study the time evolution of the lattice model we use an approximate functional RG [23] based approach which was originally developed for *open* quantum systems [24]. We establish it as a tool for studies of *closed* ones as well. This illustrates the remarkable flexibility of the functional RG approach to quantum many-body physics. For small two-particle interactions this essentially analytical approach allows controlled access to time scales large enough such that the physics is dominated by the steady state. This

complements numerical approaches which provide ‘exact’ results at small t but abruptly become unreliable beyond a characteristic time scale [25–28] which might be smaller than the one on which the steady state is reached [21].

Bosonization—The starting point of our investigation of LL universality is the exact computation of the desired observables and correlation functions within the (spinless) TL model using bosonization [6, 7, 22]. Starting out from the 1d electron gas the TL model is obtained by linearizing the single-particle dispersion and keeping only the marginal two-particle scattering terms. In contrast to earlier studies on interaction quenches in the TL model [14–21, 29–31] we consider the one with *open boundaries* at $x = 0$ and $x = L$ [11, 32]. This allows us to distinguish between bulk and boundary LL exponents [33, 34]. While the former are quadratic in the two-particle interaction the latter are linear. The model is given by the Hamiltonian

$$H_{\text{TL}} = \sum_{n=1}^{\infty} k_n \left[v_F b_n^\dagger b_n + \frac{1}{4\pi} u(k_n) (b_n^\dagger + b_n)^2 \right], \quad (1)$$

with the Fermi velocity v_F , $k_n = n\pi/L$, the two-particle potential $u(k)$, and bosonic operators $b_n^{(\dagger)}$ associated with the density of the fermions. Employing a Bogoliubov transformation H_{TL} can be written as a diagonal quadratic form in eigenmodes with (bosonic) ladder operators $\alpha_n^{(\dagger)}$ and energy $\omega_n = v_F k_n \sqrt{1 + u(k_n)/(\pi v_F)}$. The mode occupancies $\alpha_n^\dagger \alpha_n$ are independent integrals of motion. To keep the formulas transparent we here take the noninteracting canonical statistical operator ρ_c^0 as the initial state; in [35] we describe the changes when starting in the canonical state with $u_i(k) > 0$.

Using the Bogoliubov transformation and bosonization of the field operator [6, 7, 22, 32] it is straight forward to derive closed analytical expressions for the time dependence of a variety of observables and correlation functions. We exclusively consider quantities which become stationary and aim at their steady state values. Those are obtained by computing $\text{Tr} [\rho_c^0 e^{iHt} O e^{-iHt}]$ and *after* performing the thermodynamic limit taking the limit $t \rightarrow \infty$, where O stands either for an observable or the operator product defining a correlation function. We verified that the same expectation values follow from taking $\lim_{L \rightarrow \infty} \text{Tr} [\rho_{\text{GGE}} O]$, with the statistical operator $\rho_{\text{GGE}} = \exp \{ - \sum_{n>0} \eta_n \alpha_n^\dagger \alpha_n \} / Z_{\text{GGE}}$ of a nonthermal *generalized Gibbs ensemble* (GGE) [3, 14, 16, 17, 19, 36] and Z_{GGE} determined such that $\text{Tr} \rho_{\text{GGE}} = 1$. The η_n are fixed by requiring $\text{Tr} [\alpha_n^\dagger \alpha_n \rho_{\text{GGE}}] = \text{Tr} [\alpha_n^\dagger \alpha_n \rho_c^0]$.

Despite being described by the density matrix ρ_{GGE} the steady state of the TL model is ‘critical’, that is characterized by LL power laws. This is known from quenches in the translational invariant TL model [14–16, 19] and intimately linked to the mode index n dependence of η_n/ω_n . Table I contains the $T = 0$ scaling exponents in the nonequilibrium steady state of interest to us. They

observable/correl. funct.	variable	eq. exp.	steady-state exp.
access density Δn	x	$-K$	$-(K^2 + 1)/2$
local DOS ρ	ω	$K^{-1} - 1$	$(K^{-2} - 1)/2$
bulk χ at $\omega = 0$	$q - 2k_F$	$2(K - 1)$	$K^2 - 1$

TABLE I. Equilibrium and steady-state scaling exponents.

can all be expressed in terms of the models LL parameter $K = [1 + u(0)/(\pi v_F)]^{-1/2}$ but differ from the corresponding known equilibrium exponents (third column) [6–11]. In the next section we directly compare the decay of the densities Friedel oscillations off the boundary in the steady state of a microscopic lattice model with the TL model prediction (first row of Table I).

The scaling behavior of the bulk density response $\chi(q, \omega = 0)$ (last row of Table I) allows us to make predictions for how the steady state reacts to a single impurity. For repulsive interactions $K^2 - 1 < 0$ and χ diverges for $q \rightarrow 2k_F$. As in equilibrium even a weak single local impurity strongly disturbs the homogenous system. When applying an infinitesimal bias voltage V across the impurity the conductance $G = dI^{\text{st}}/dV$ (with the stationary current I^{st}) is expected to scale as $G_0 - G(T) \sim T^{K^2-1}$, with the constant homogenous chain conductance G_0 . In the following we denote G as the *steady-state linear conductance*. The nonequilibrium nature of the considered state stems dominantly from the interaction quench and not the small $|V|$. The power law holds as long as the right hand side stays small, that is for not too small T . Using the language of equilibrium RG this indicates that the perfect chain fixed point is unstable. In contrast, the open chain one is stable as follows from the scaling of the local density of states (DOS; second row of Table I). Fermis Golden Rule-like arguments lead to the vanishing of the tunneling conductance $G \sim T^{K^2-1}$ across a weak link connecting two semi-infinite chains with suppressed DOS. These arguments do not rule out intermediate impurity fixed points. As in equilibrium [11] excluding those requires a method beyond perturbation theory in the impurity strength and the weak link hopping [12, 13]. Provided the concept of LL universality holds for the steady state we expect to find those weak and strong impurity scaling laws of $G(T)$ for a lattice model with the K of the model considered. Using a one-parameter scaling ansatz and our nonperturbative RG we investigate the possibility of intermediate impurity fixed points.

Microscopic model—We consider the lattice model of spinless fermions with nearest-neighbor hopping J as well as interaction U and open boundaries terminating the N -site chain given by

$$H_{\text{LM}}(U) = \sum_{j=1}^{N-1} \left[-J c_j^\dagger c_{j+1} + \text{H.c.} + U c_j^\dagger c_j c_{j+1}^\dagger c_{j+1} \right] \quad (2)$$

in standard second quantized notation. In equilibrium

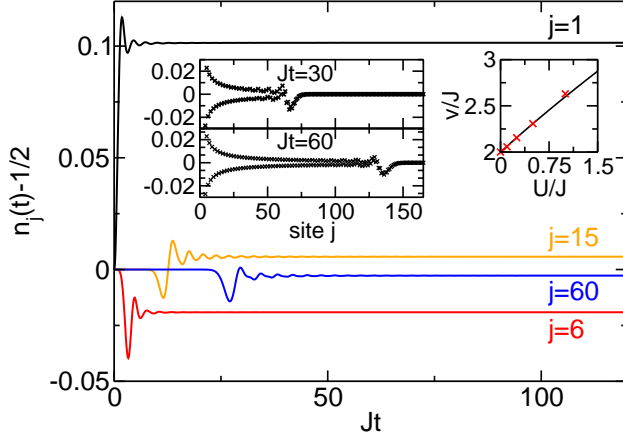


FIG. 1. (Color online) Functional RG data for the time evolution of $n_j(t) - \nu$ at half filling $\nu = 1/2$ after a quench in the interaction amplitude to $U/J = 0.5$ for $N = 10^3$, $T = 0$, and different sites j . Left inset: Friedel oscillations induced by the boundary and the propagation of a main signal from the boundary to $j \approx vt$ for two values of t . Right inset: Velocity of the main signal for different U (symbols). The exact Bethe ansatz v (line) is in excellent agreement with our data.

the model is (A) Bethe ansatz solvable and (B) shows universal LL physics with K and v exactly known [8]. It is commonly believed that because of (A) the steady state after an interaction quench is described by a GGE but the corresponding ρ_{GGE} was neither constructed nor was a proof of its existence given. Our analysis does not rely on any such assumption. When discussing the impurity physics H_{LM} is supplemented by a hopping impurity $H_{\text{imp}} = hc_{N/2}^\dagger c_{N/2+1} + \text{H.c.}$ of strength $h \in [0, J]$ located in the middle of the chain. To compute the time evolution of the density n_j as well as the conductance we use an approximate functional RG [23] based approach originally developed to investigate the nonequilibrium dynamics of open systems [24]. A related method was earlier shown to capture the equilibrium LL properties of inhomogeneous lattice models [12, 13] including the characteristic power-law scaling, with exponents agreeing to the exact ones to leading order in U . Our approach is essentially analytical but in its last step requires the numerical solution of a set of $\mathcal{O}(N \cdot N_t)$ coupled differential equations, with the number of time steps N_t , and the computation of matrix exponentials of $N \times N$ -matrices [35].

In Fig. 1 we show the access density $n_j(t) - \nu$ for fixed j starting out of the noninteracting impurity free ground state ($T = 0$) [35]. Despite the open boundaries for filling $\nu = 1/2$ the initial state has a homogeneous density $n_j(t=0) = 1/2$ [34]. We can reach times of the order of a few $10^2/J$ which has to be contrasted to other commonly employed methods which become unreliable for times of the order of $10/J$ [21]. As shown in the main plot and the left inset a prominent signal originating from the left boundary travels through the system. A similar one is generated at the right one. For a spatial region in which

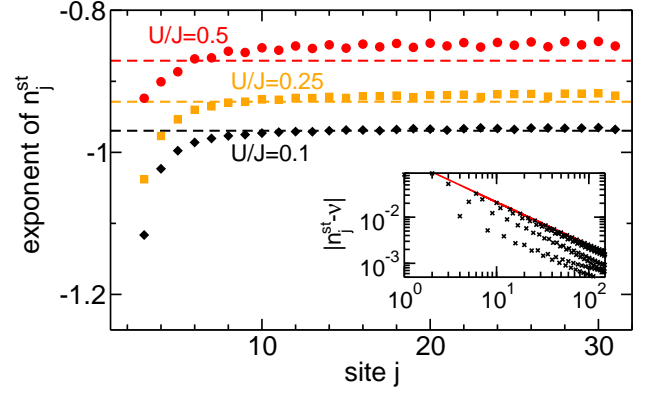


FIG. 2. (Color online) Functional RG data for the effective exponent of the Friedel oscillations of the steady-state density n_j^{st} for $\nu = 1/2$, $N = 10^3$, and $T = 0$ determined by taking the log-derivative. The predictions from the TL model with the exact lattice model K (dashed lines) are consistent with our results. The inset shows $|n_j^{\text{st}} - \nu|$ at $\nu = 0.375$ and $U/J = 0.25$ (symbols). The line is the TL model prediction.

the left signal passed through and the right one did not enter yet the density becomes stationary. The physics for $t \approx 10^2/J$ and j up to $\mathcal{O}(10^2)$ is thus dominated by the steady state and does barely suffer from finite size effects. The two main signals propagate with the LL velocity v [37–39], with our method providing an excellent approximation to the exact v (right inset of Fig. 1).

In analogy to the interacting ground state (see e.g. [12]) the stationary density n_j^{st} shows Friedel oscillations with frequency $2k_F$ (see the $j < 80$ region of the lower part of the left inset of Fig. 1). We next analyze their decay. Figure 2 shows the log-derivative of $|n_j^{\text{st}} - 1/2|$, that is an effective exponent. The dashed lines is the prediction from the TL model of Table I with the exact lattice model K . Our data are consistent with a power-law decay and the TL model exponent. This finding is our first indication of LL universality of the steady state. The differences between the exact exponent and our result is of order U^2 . On the right hand side of our RG flow equations we do not fully capture terms $\sim U^2$ and thus control exponents only to order U . The discussed behavior is not restricted to the case of half filling. The inset of Fig. 2 shows $|n_j^{\text{st}} - \nu|$ for $\nu = 0.375$ on a log-log scale and the corresponding TL model prediction as the envelope.

To compute the steady-state linear conductance of the lattice model we take the canonical density matrix ρ_c^0 (with $T > 0$) corresponding to $H_{\text{LM}}(U = 0) + H_{\text{imp}}$ as the initial state. The time evolution is performed with $H_{\text{LM}}(U > 0) + H_{\text{imp}}$ supplemented by onsite energies $V/2$ ($-V/2$) for all $j \leq N/2$ ($j > N/2$). Thus not only the two-particle interaction but in addition a small bias voltage V is abruptly turned on at $t = 0$. The current $I(t)$ across the impurity bond is computed [35]. Following the same reasoning as for the density I becomes stationary for t of the order of $10^2/J$. We take V to be the smallest

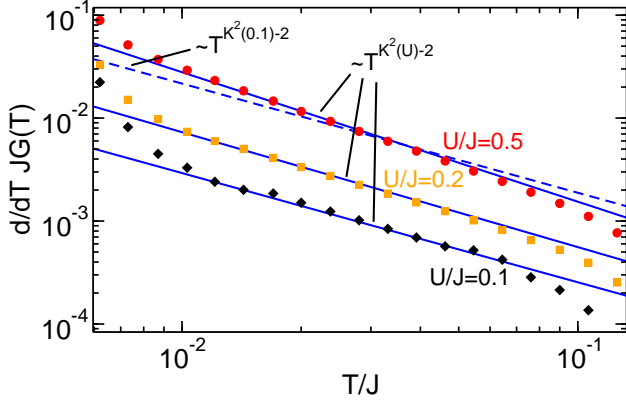


FIG. 3. (Color online) Functional RG data for the temperature derivative of the steady-state linear conductance of our lattice model for a weak impurity $h/J = 0.05$, filling $\nu = 1/2$, and $N = 10^3$ (symbols). The prediction from the TL model with the exact lattice model K is shown as the solid lines. To emphasize the sizable differences in the exponents we have added a power law with the $U/J = 0.1$ exponent as the dashed line to the $U/J = 0.5$ data.

energy scale of the problem (typically $V = 10^{-3}J$) to ensure that we are in the linear regime $I^{\text{st}} = GV$. For $T \gtrsim J$ we find independent of h , U , and ν , $G(T) \sim T^{-1}$ [13] which is a band effect (see the inset of Fig. 4). The universal scaling of the conductance discussed in the last section can only be expected for $T \ll J$.

We first analyze the case of weak impurities. To eliminate the constant G_0 we take the derivative of G with respect to T . Based on our above considerations we expect to find $dG/dT \sim T^{K^2-2}$; see Fig. 3. Over roughly one order of magnitude the functional RG data follow the TL model prediction with the exact K of our lattice model. The deviations for $T/J > 0.1$ indicate the crossover to the nonuniversal $G(T) \sim T^{-1}$ regime. The deviations for $T/J < 0.01$ have two reasons. As discussed above the scaling only holds as long as T does not become too small. Furthermore, the energy level spacing $\delta_N = v_F/N$ ($= 2 \cdot 10^{-3}J$ for the parameters of the plot) is an energy scale of the problem which cuts off any universal behavior [12, 13]. This is an artefact of our treatment of finite systems. For small h and $T/J \in [0.1, 0.005]$, $G_0 - G(T) \ll 1$. Our analysis thus requires very accurate data. To minimize the error due to small residual oscillations of $I(t)$ present even for t of the order of $10^2/J$ we averaged the data at large t over a small time interval.

In the inset of Fig. 4 we present our results for $G(T)$ across a strong impurity ($h/J = 0.9$). Even without any t averaging our data are accurate enough such that the log-derivative, that is the effective exponent, gives a smooth curve. The data clearly show the crossover from the nonuniversal T^{-1} behavior at large T to the TL model prediction T^{K^2-1} at low ones down to the cutoff scale δ_N . In the limits of strong and weak impurities our results for the linear conductance of the lattice model thus

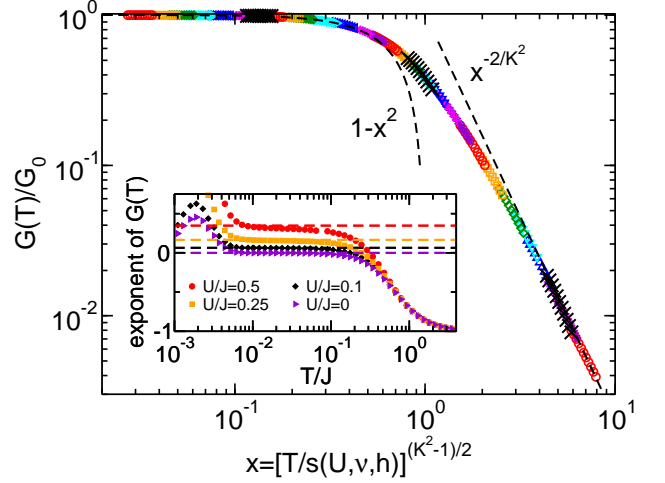


FIG. 4. (Color online) Functional RG data for the one-parameter scaling of $G(T)$ of the lattice model for $U/J = 0.5$, $\nu = 1/2$, and $N = 10^3$. Different symbols stand for different h increasing from left to right. No fixed point in between the perfect and the open chain ones exist. The crosses were computed for $U/J = 0.85$, $\nu = 1/4$ giving the same K . The scaling function thus depends on U and ν only via K [11]. The prediction of the TL model for $x \rightarrow 0$ and $x \rightarrow \infty$ with the exact lattice model K is shown as dashed lines. Inset: the effective exponent of $G(T)$ for a strong impurity $h/J = 0.9$ determined by a log-derivative. Dashed lines show the prediction of the TL model with the exact lattice model K .

agree to the TL model prediction providing the second indication of LL universality of the steady state.

We finally show that in the steady state of the lattice model no fixed point in between the perfect and the open chain ones exist. To this end we compute $G(T)$ for a variety of h at fixed U and ν . Using a one-parameter scaling ansatz of the form $G(T) = \bar{G}(x)$ [11, 13], with $x = (T/s)^{(K^2-1)/2}$ and the nonuniversal scale $s(U, \nu, h)$, all data can be collapsed on a single curve continuously connecting the weak ($x \rightarrow 0$) and strong ($x \rightarrow \infty$) impurity fixed points; see the main plot of Fig. 4. We conclude that the impurity physics of the LL steady state is similar to the equilibrium one [11].

Outlook—We provided evidence that the steady state of an interacting 1d lattice model after a quantum quench shows LL universality and that the impurity physics of the LL steady state is similar to the one in equilibrium. Both should be confirmed by studying other models of interacting fermions using alternative methods. In particular, it would be interesting to investigate if the ‘critical’ LL physics can be found in the steady state of models which are not Bethe ansatz solvable (‘nonintegrable’). For the asymptotic time dependence indications of universal LL power laws were found [21]. Studying ‘nonintegrable’ Hamiltonians obtained from the one Eq. (2) by adding further terms is beyond the current possibilities of our method as we would have to give up the crucial requirement of small nearest neighbor interactions.

Acknowledgments—We thank S. Andergassen C. Karrasch, K. Schönhammer, D. Schuricht, and G. Uhrig for discussions as well as S. Blügel and the Jülich Supercomputing Centre for access to the JuDGE GPU cluster. This work was supported by the DFG via FOR 723.

-
- [1] I. Bloch, J. Dalibard, and W. Zwerger, *Rev. Mod. Phys.* **80**, 885 (2008).
 - [2] A. Polkovnikov, K. Sengupta, A. Silva, and M. Vengalattore, *Rev. Mod. Phys.* **83**, 863 (2011).
 - [3] M. Rigol, V. Dunjko, V. Yurovsky, and M. Olshanii, *Phys. Rev. Lett.* **98**, 050405 (2007).
 - [4] T. Barthel and U. Schollwöck, *Phys. Rev. Lett.* **100**, 100601 (2008).
 - [5] M. Fagotti and F.H.L. Essler, arXiv:1302.6944 (2013).
 - [6] T. Giamarchi, *Quantum Physics in One Dimension* (New York: Oxford University Press, 2003).
 - [7] K. Schönhammer in *Interacting Electrons in Low Dimensions* ed. by D. Baeriswyl (Dordrecht: Kluwer Academic Publishers, 2005).
 - [8] F.D.M. Haldane, *Phys. Rev. Lett.* **45**, 1358 (1980).
 - [9] J. Sólyom, *Adv. Phys.* **28**, 209 (1979).
 - [10] A. Luther and I. Peschel, *Phys. Rev. B* **9**, 2911 (1974).
 - [11] C.L. Kane and M.P.A. Fisher, *Phys. Rev. Lett.* **68**, 1220 (1992).
 - [12] S. Andergassen, T. Enss, V. Meden, W. Metzner, U. Schollwöck, and K. Schönhammer, *Phys. Rev. B* **70**, 075102 (2004).
 - [13] T. Enss, V. Meden, S. Andergassen, X. Barnabe-Therault, W. Metzner, and K. Schönhammer, *Phys. Rev. B* **71**, 155401 (2005).
 - [14] M.A. Cazalilla, *Phys. Rev. Lett.* **97**, 156403 (2006).
 - [15] G.S. Uhrig, *Phys. Rev. A* **80**, 061602 (2009).
 - [16] A. Iucci and M.A. Cazalilla, *Phys. Rev. A* **80**, 063619 (2009).
 - [17] D.M. Kennes and V. Meden, *Phys. Rev. B* **82**, 085109 (2010).
 - [18] B. Dóra, M. Haque, and G. Zaránd, *Phys. Rev. Lett.* **106**, 156406 (2011).
 - [19] J. Rentrop, D. Schuricht, and V. Meden, *New J. Phys.* **14**, 075001 (2012).
 - [20] A. Mitra and T. Giamarchi, *Phys. Rev. Lett.* **107**, 150602 (2011).
 - [21] C. Karrasch, J. Rentrop, D. Schuricht, and V. Meden, *Phys. Rev. Lett.* **109**, 126406 (2012).
 - [22] J. von Delft and H. Schoeller, *Annalen der Physik* **7**, 225 (1998).
 - [23] W. Metzner, M. Salmhofer, C. Honerkamp, V. Meden, and K. Schönhammer, *Rev. Mod. Phys.* **84**, 299 (2012).
 - [24] D.M. Kennes, S.G. Jakobs, C. Karrasch, and V. Meden, *Phys. Rev. B* **85**, 085113 (2012).
 - [25] U. Schollwöck, *Ann. Phys.* **326**, 96 (2011).
 - [26] G. Vidal, *Phys. Rev. Lett.* **93**, 040502 (2004).
 - [27] S. R. White and A. E. Feiguin, *Phys. Rev. Lett.* **93**, 076401 (2004).
 - [28] A. Daley, C. Kollath, U. Schollwöck, and G. Vidal, *J. Stat. Mech.*, P04005 (2004).
 - [29] S.A. Hamerla and G.S. Uhrig, arXiv:1207.2006 (2012).
 - [30] F. Pollmann, M. Haque, and B. Dóra, *Phys. Rev. B* **87**, 041109(R) (2013).
 - [31] B. Dóra, F. Pollmann, and G. Zaránd, arXiv:1303.7169 (2013).
 - [32] M. Fabrizio and A. Gogolin, *Phys. Rev. B* **51**, 17827 (1995).
 - [33] A.E. Mattsson, S. Eggert, and H. Johannesson, *Phys. Rev. B* **56**, 15615 (1997).
 - [34] V. Meden, W. Metzner, U. Schollwöck, O. Schneider, T. Stauber, and K. Schönhammer, *Eur. Phys. J. B* **16**, 631 (2000).
 - [35] See the attached Supplementary Material.
 - [36] F.H.L. Essler, S. Evangelisti, and M. Fagotti, *Phys. Rev. Lett.* **109**, 247206 (2012).
 - [37] P. Calabrese and J. Cardy, *J. Stat. Mech.* P10004 (2007).
 - [38] S. Langer, F. Heidrich-Meisner, J. Gemmer, I.P. McCulloch, and U. Schollwöck, *Phys. Rev. B* **79**, 214409 (2009).
 - [39] M. Ganahl, E. Rabel, F.H.L. Essler, and H.G. Evertz, *Phys. Rev. Lett.* **108**, 077206 (2012).

Supplementary Material to 'Luttinger liquid properties of the steady state after a quantum quench'

D.M. Kennes and V. Meden

*Institut für Theorie der Statistischen Physik, RWTH Aachen University and
JARA—Fundamentals of Future Information Technology, 52056 Aachen, Germany*

BOSONIZATION

To compute observables and correlation functions in the steady state of the Tomonaga-Luttinger (TL) model with open boundaries after an interaction quench we use 'open boundary bosonization' for the Hamiltonian and the field operator [1–4]. We are interested in the scaling behavior with all energy scales send to zero and all length scales send to infinity. Thus subtleties resulting out of the momentum dependence of the two-particle potential $u(k)$ become irrelevant [5, 6] and the ultraviolet regularization can be implemented at will. To illustrate the procedure we consider the density $n(x, t)$. We first study the quench from $u_i(k) = 0$ to $u_f(k) = u(k)$. For simplicity we focus on temperature $T = 0$. The density is given by the Green function

$$iG_t(x, x) = \langle \text{vac}(b) | e^{iH_{\text{TL}}t} \psi^\dagger(x) \psi(x) e^{-iH_{\text{TL}}t} | \text{vac}(b) \rangle,$$

with the noninteracting ground state $|\text{vac}(b)\rangle$ which corresponds to the vacuum with respect to the b 's (in the same notation as in the main text). The fields $\psi^{(\dagger)}(x)$ contain the open boundary conditions. Using auxiliary fields $\tilde{\psi}^{(\dagger)}(x)$ which are identical to the ones obtained for periodic boundary conditions [7–9] and are e.g. given in Eqs. (18)–(20) of Ref. [6], the Green function reads

$$\begin{aligned} iG_t(x, x) = & \frac{1}{2} \left[\langle \text{vac}(b) | e^{iH_{\text{TL}}t} \tilde{\psi}^\dagger(x) \tilde{\psi}(x) e^{-iH_{\text{TL}}t} | \text{vac}(b) \rangle \right. \\ & + \langle \text{vac}(b) | e^{iH_{\text{TL}}t} \tilde{\psi}^\dagger(-x) \tilde{\psi}(-x) e^{-iH_{\text{TL}}t} | \text{vac}(b) \rangle \\ & - \langle \text{vac}(b) | e^{iH_{\text{TL}}t} \tilde{\psi}^\dagger(x) \tilde{\psi}(-x) e^{-iH_{\text{TL}}t} | \text{vac}(b) \rangle \\ & \left. - \langle \text{vac}(b) | e^{iH_{\text{TL}}t} \tilde{\psi}^\dagger(-x) \tilde{\psi}(x) e^{-iH_{\text{TL}}t} | \text{vac}(b) \rangle \right]. \end{aligned}$$

Those expectation values can be computed following the usual steps [7–9] which involve the multiple use of the Bogoliubov transformation $b_n = c(k_n)\alpha_n + s(k_n)\alpha_n^\dagger$ and the Baker-Campbell-Hausdorff relation. The coefficients $c(k_n)$ and $s(k_n)$ depend on the two-particle potential $u(k_n)$ and are e.g. given in Eq. (9) of Ref. [6]. The first two terms of the Green function provide the homogeneous background density while the latter two oscillate in space with frequency $2k_F$ —they contain the Friedel oscillations induced by the boundaries. After taking the thermodynamic limit and the limit $t \rightarrow \infty$ we find for the steady-state access density

$$\Delta n^{\text{st}}(x) \sim x^{-[c^2(0)+s^2(0)][c(0)+s(0)]} \cos(2k_F x). \quad (1)$$

At zero momentum the coefficients of the Bogoliubov transformation can be expressed in terms of the models Luttinger liquid (LL) parameter K given in the main text as

$$s^2(0) = \frac{1}{4}(K + K^{-1} - 2), \quad c^2(0) = \frac{1}{4}(K + K^{-1} + 2). \quad (2)$$

Using those relations the exponent of Eq. (1) can be written as $-(K^2 + 1)/2$ (see Table I of the main text). The other scaling exponents of the last column of Table I of the main text can be obtained in a similar fashion.

In any (equilibrium) LL the LL parameter is given by

$$K = 1 - \tilde{U} + \mathcal{O}(\tilde{U}^2), \quad (3)$$

where \tilde{U} is a dimensionless measure for the interaction strength; e.g. $\tilde{U} = u(0)/(2\pi v_F)$ for the TL model and $\tilde{U} = U[1 - \cos(2k_F)]/[2\pi J \sin(k_F)]$ for our lattice model at filling $\nu = k_F/\pi$. Using this expansion it is evident that all scaling exponents discussed by us (see Table I of the main text) have a leading order contribution in \tilde{U} . This is crucial as within our approximate treatment of the lattice model we control exponents only to leading order [10].

We next briefly discuss the case when starting in the ground state of H_{TL} with $u_i(k) > 0$ and performing the time evolution with a different interaction $u_f(k) > 0$; all quantities depending on the interaction strength acquire indices i or f. We have to consider two Bogoliubov transformations [corresponding to the transformations from zero interaction to $u_{i/f}(k)$] and two sets of eigenmode ladder operators. The initial state is the vacuum with respect to one of those while the Hamiltonian with which the time evolution is performed is a diagonal quadratic form in the other one. Repeatedly applying the Bogoliubov transformations and the Baker-Campbell-Hausdorff relation gives for the steady-state access density

$$\Delta n^{\text{st}}(x) \sim x^{-\gamma} \cos(2k_F x), \quad (4)$$

with the scaling exponent

$$\begin{aligned} \gamma = K_f \left[1 + \frac{1}{8}(K_i + K_i^{-1} - 2)(K_f + K_f^{-1} + 2) \right. \\ \left. - \frac{1}{4}(K_i - K_i^{-1})(K_f - K_f^{-1}) \right. \\ \left. + \frac{1}{8}(K_i + K_i^{-1} + 2)(K_f + K_f^{-1} - 2) \right]. \quad (5) \end{aligned}$$

For $K_i = 0$, that is if we start in the noninteracting ground state, it becomes equal to $(K_f^2 + 1)/2$ (see Table I

of the main text). Using the expansion Eq. (3) it is easy to see that γ and $(K_f^2 + 1)/2$ agree to leading order in the two-particle interaction, that is U_i only contributes to order U_i^2 and $U_f U_i$ or higher. To leading order in the interaction strength the scaling exponent of the density is thus exclusively given by U_f . The same holds for the other exponents considered by us (see Table I of the main text). In our computations for the lattice model we control exponents only to leading order which explains why in the main text we exclusively consider quenches out of the noninteracting ground state.

FUNCTIONAL RENORMALIZATION GROUP

In the main text we use the functional renormalization group (RG) approach [10] to study the relaxation dynamics and the steady state of a closed many-body system described by the lattice model of spinless fermions with nearest neighbor hopping and interaction. Compared to the functional RG approach to time evolution for open quantum systems introduced in Ref. [11], some minor amendments need to be made. Those are outlined next.

We can treat Hamiltonians of the form

$$H = H_0 + H_{\text{int}}, \quad (6)$$

$$H_0 = \sum_{ij} \epsilon_{ij} c_i^\dagger c_j, \quad (7)$$

$$H_{\text{int}} = \frac{1}{4} \sum_{ijkl} \bar{u}_{ijkl} c_i^\dagger c_j^\dagger c_l c_k \quad (8)$$

written in standard second quantization. Here \bar{u}_{ijkl} is the antisymmetrized two-particle interaction. The indices i, j, \dots stand for the quantum numbers, e.g. the N Wannier states in our lattice model. The Hamiltonian Eq. (2) of the main text falls into this class of general Hamiltonians. We assume an initial density matrix

$$\rho^0 = \frac{e^{\sum_{ij} \beta_{ij} c_i^\dagger c_j}}{\text{Tr} \left[e^{\sum_{ij} \beta_{ij} c_i^\dagger c_j} \right]} \quad (9)$$

which allows for the application of Wick's theorem. In the main text we always choose the noninteracting canonical statistical operator $\rho^0 = \rho_c^0 = \exp(-\beta H_0) / \text{Tr}[\exp(-\beta H_0)]$. The two-particle interaction is treated approximately using functional RG in its lowest order truncation [10]. We introduce a cutoff in the noninteracting Keldysh [12] Green functions g (as motivated in Ref. [11]) by

$$g^{\text{ret},\Lambda}(t, t') = -i\Theta(t - t') e^{-i\epsilon(t-t')} e^{-i\Lambda(t-t')} \quad (10)$$

$$= [g^{\text{adv},\Lambda}(t', t)]^\dagger, \quad (11)$$

$$g^{\text{K},\Lambda}(t, t') = -ig^{\text{ret},\Lambda}(t, 0)(1 - 2\bar{n})g^{\text{adv},\Lambda}(0, t'), \quad (12)$$

with ϵ being the $N \times N$ matrix with entries ϵ_{ij} and $\bar{n}_{ii'} = \text{Tr} [\rho^0 d_i^\dagger d_i]$. The self-energy is obtained by solving a set of coupled differential flow equations

$$\begin{aligned} \partial_\Lambda \Sigma_{i_1 i_1'}^{\text{ret},\Lambda}(t', t) &= \partial_\Lambda \Sigma_{i_1 i_1'}^{\text{adv},\Lambda}(t', t) \\ &= - \sum_{i_2, i_2'} S_{i_2' i_2}^{\text{K},\Lambda}(t, t) (-i\bar{u}_{i_1 i_2 i_2' i_1'}(t)) \delta(t' - t), \end{aligned} \quad (13)$$

$$\partial_\Lambda \Sigma^{\text{K},\Lambda} = 0, \quad (14)$$

with the initial conditions at $\Lambda = \infty$

$$\Sigma_{i'i}^{\text{ret},\Lambda=\infty}(t', t) = \frac{1}{2} \delta(t - t') \sum_j \bar{u}_{i' j i j}, \quad (15)$$

$$\Sigma_{i'i}^{\text{K},\Lambda=\infty}(t', t) = 0. \quad (16)$$

The right hand sides of the flow equations contain

$$S^{\text{K},\Lambda} = \partial_\Lambda^* G^{\text{K},\Lambda}, \quad (17)$$

with the full cutoff dependent Keldysh component of the Green function

$$G^{\text{K},\Lambda}(t, t') = -iG^{\text{ret},\Lambda}(t, 0)(1 - 2\bar{n})G^{\text{adv},\Lambda}(0, t'). \quad (18)$$

The star differential operator ∂_Λ^* acts only on the free Green function $g^{\text{ret}/\text{adv},\Lambda}$, not on Σ^Λ , in the Dyson series expansion $G^{\text{ret}/\text{adv},\Lambda} = g^{\text{ret}/\text{adv},\Lambda} + g^{\text{ret}/\text{adv},\Lambda} \Sigma^\Lambda g^{\text{ret}/\text{adv},\Lambda} + \dots$ used to calculate $G^{\text{ret}/\text{adv},\Lambda}$. An approximation to the self-energy of the cutoff-free problem is obtained at $\Lambda = 0$.

We can calculate $G^{\text{K},\Lambda}(t, t')$ very efficiently by using an iterative procedure. First, we discretize time in steps such that during one small step Δt the time dependent self-energy can be set constant. For our results shown in the main text we made sure that Δt is always chosen small enough such that further reducing it does not lead to any changes visible on the scale of the respective plots. We use

$$\begin{aligned} G^{\text{ret},\Lambda}(t, t') G^{\text{ret},\Lambda}(t', t'') \\ = -i\Theta(t - t') \Theta(t' - t'') G^{\text{ret},\Lambda}(t, t''). \end{aligned} \quad (19)$$

$$G^{\text{ret},\Lambda}(t, t') = [G^{\text{adv},\Lambda}(t', t)]^\dagger, \quad (20)$$

to write $G^{\text{ret}}(t, t')$ as a product of Green functions

$$G^{\text{ret},\Lambda}(t_1 + \Delta t, t_1) = -ie^{-i[\epsilon + \bar{\Sigma}^{\text{ret},\Lambda}(t_1)]\Delta t} e^{-i\Lambda(t-t')}, \quad (21)$$

where $\bar{\Sigma}^{\text{ret},\Lambda}(t_1)$ is the self-energy time averaged over the interval $(t_1, t_1 + \Delta t)$. The interacting Keldysh Green function $G^{\text{K},\Lambda}(t, t)$ can then be found iteratively employing

$$\begin{aligned} G^{\text{K},\Lambda}(t + \Delta t, t + \Delta t) \\ = G^{\text{ret},\Lambda}(t + \Delta t, t) G^{\text{K},\Lambda}(t, t) G^{\text{ret},\Lambda}(t, t + \Delta t), \end{aligned} \quad (22)$$

$$G^{\text{K},\Lambda}(0, 0) = -i(1 - 2\bar{n}). \quad (23)$$

In every time step two matrix exponentials of $N \times N$ matrices have to be performed and multiplied with the Keldysh component of the Green function of the previous one. This renders the problem a natural candidate for graphics processing unit (GPU) supported algorithms. We use such to compute the results shown in the main text. The number N_t of time steps needed to obtain sufficient accuracy (and resolution) as well as to reach times which are large enough such that the physics is dominated by the steady state enters the number of equations to be solve. For the Hamiltonian considered in the main text we solve sets of $(3N-2)N_t$ coupled differential equations. Due to the nearest neighbor structure of the interaction $3N-2$ components of the self energy flow for each of the N_t time steps. Typical numbers considered are $N = 1000$ lattice sites and $N_t = 1600$ time steps.

COMPUTING OBSERVABLES

An approximation for the occupancy of site j can directly be obtained from the Keldysh Green function at the end of the RG flow as

$$n_j(t) = \frac{1}{2} - \frac{i}{2} G_{jj}^{K, \Lambda=0}(t, t). \quad (24)$$

To calculate the current flowing from the left to the right half of the lattice in our microscopic model of interacting spinless fermions, we need to determine

$$I(t) = -\frac{d}{dt} \langle N_L(t) \rangle_{\rho^0}, \quad (25)$$

where N_L is defined as $N_L(t) = \sum_{j=1}^{N/2} n_j(t)$, with $n_j = c_j^\dagger c_j$ being the occupancy operator of site j [13] and $\langle \dots \rangle_{\rho^0}$ denotes the expectation value with respect to ρ^0 . For simplicity we assume an even number of lattice sites

N . Furthermore, we use

$$I(t) = -i \langle [H, N_L](t) \rangle_{\rho^0} = (h - J) G_{N/2N/2+1}^{<}(t, t) + \text{c.c.} \quad (26)$$

with $G_{N/2N/2+1}^{<}(t, t)$ being the equal-time lesser Green function of the interacting system [12]. The functional RG method used here provides an approximation for this given by

$$G_{ij}^{<, \Lambda=0}(t, t) = \frac{1}{2} \left[i - G_{ij}^{K, \Lambda=0}(t, t) \right]. \quad (27)$$

Therefore, plugging this lesser Green function into Eq. (26) allows to compute an approximation to the current and from this the conductance.

-
- [1] M. Fabrizio and A. Gogolin, Phys. Rev. B **51**, 17827 (1995).
 - [2] A.E. Mattsson, S. Eggert, and H. Johannesson, Phys. Rev. B **56**, 15615 (1997).
 - [3] V. Meden, W. Metzner, U. Schollwöck, O. Schneider, T. Stauber, and K. Schönhammer, Eur. Phys. J. B **16**, 631 (2000).
 - [4] S. Grap and V. Meden, Phys. Rev. B **80**, 193106 (2009).
 - [5] V. Meden, Phys. Rev. B **60**, 4571 (1999).
 - [6] J. Rentrop, D. Schuricht, and V. Meden, New J. Phys. **14**, 075001 (2012).
 - [7] J. von Delft and H. Schoeller, Annalen der Physik **7**, 225 (1998).
 - [8] T. Giamarchi, *Quantum Physics in One Dimension* (New York: Oxford University Press, 2003).
 - [9] K. Schönhammer in *Interacting Electrons in Low Dimensions* ed. by D. Baeriswyl (Dordrecht: Kluwer Academic Publishers, 2005).
 - [10] W. Metzner, M. Salmhofer, C. Honerkamp, V. Meden, and K. Schönhammer, Rev. Mod. Phys. **84**, 299 (2012).
 - [11] D.M. Kennes, S.G. Jakobs, C. Karrasch, and V. Meden, Phys. Rev. B **85**, 085113 (2012).
 - [12] J. Rammer, *Quantum Field Theory of Non-equilibrium States* (Cambridge University Press, Cambridge, 2007).
 - [13] Y. Meir and N.S. Wingreen, Phys. Rev. Lett. **68**, 2512 (1992).